Elucidating membrane structure and protein behavior using giant plasma membrane vesicles

Erdinc Sezgin[1,2], Hermann-Josef Kaiser[3], Tobias Baumgart[4], Petra Schwille[1], Kai Simons[2] & Ilya Levental[2]

[1]Biophysics/BIOTEC, Technische Universität Dresden, Dresden, Germany. [2]Max Planck Institute for Molecular Cell Biology and Genetics, Dresden, Germany. [3]Max Delbrück Center for Molecular Medicine, Berlin, Germany. [4]Department of Chemistry, University of Pennsylvania, Philadelphia, Pennsylvania, USA. Correspondence should be addressed to I.L. (levental@mpi-cbg.de).

Published online 3 May 2012; doi:10.1038/nprot.2012.059

The observation of phase separation in intact plasma membranes isolated from live cells is a breakthrough for research into eukaryotic membrane lateral heterogeneity, specifically in the context of membrane rafts. These observations are made in giant plasma membrane vesicles (GPMVs), which can be isolated by chemical vesiculants from a variety of cell types and microscopically observed using basic reagents and equipment available in any cell biology laboratory. Microscopic phase separation is detectable by fluorescent labeling, followed by cooling of the membranes below their miscibility phase transition temperature. This protocol describes the methods to prepare and isolate the vesicles, equipment to observe them under temperature-controlled conditions and three examples of fluorescence analysis: (i) fluorescence spectroscopy with an environment-sensitive dye (laurdan); (ii) two-photon microscopy of the same dye; and (iii) quantitative confocal microscopy to determine component partitioning between raft and nonraft phases. GPMV preparation and isolation, including fluorescent labeling and observation, can be accomplished within 4 h.

INTRODUCTION

Background

The proposal of functional rafts in eukaryotic membranes[1] prompted a period of extensive research, revealing many physiological contexts that appear to use this mechanism of membrane organization for modulation of cell function. The modern conception of this phenomenon[2] is that preferential associations between raft lipids (i.e., sterols, glycosylated sphingolipids and lipids with saturated acyl chains) and certain proteins (saturated lipid anchored-proteins, as well as some transmembrane ones) promote lateral heterogeneity and segregation in the plane of the membrane. This heterogeneity can be manifested in a hierarchy of organizational states, from molecular-level complexes[3,4] and functional domains on the order of hundreds of nanometers[5] in live cells to microscopic phases[6,7] in isolated membrane systems—the specific state of any given membrane depends on a complex combination of its physical properties (e.g., temperature) and biochemical composition.

The recent discovery of phase separation in GPMVs isolated directly from live cells has convincingly validated the raft hypothesis by confirming its central tenet, i.e., the capacity of eukaryotic membranes for forming coexisting liquid domains[6]. Nevertheless, the precise nature of rafts' mechanistic involvement in specific cell functions remains speculative. To address this shortcoming, GPMVs comprise an intermediate model system which maintains the compositional complexity and protein content of biological membranes and is capable of forming coexisting, microscopic, lipid-driven domains without the many confounding variables (protein synthesis and active transport, cytoskeletal support, active signaling networks and so on) of live cells. These advantages combine to make GPMVs a versatile tool for quantitative investigation of raft-associated phenomena, specifically the structure and physical properties of coexisting domains, protein partitioning between them and domain-dependent protein and lipid function.

Plasma membrane vesicles

Although the observation of phase separation in GPMVs has recently invigorated the raft field, chemically induced plasma membrane vesiculation was first observed in the 1970s (ref. 8). This protocol produces efficient yields of large (up to 10 μm), nearly pure plasma membrane vesicles without any internal membranous structures observable by electron microscopy (EM); indeed, there are no EM-discernible intravesicular structures, suggesting the absence of assembled cytoskeleton or nuclear material[9]. Despite these advantages of yields and purities, PMVs were largely ignored as a plasma membrane model system for biochemical investigation, likely due to the chemical modifications inherent in isolation. Exceptions included the groups of Baird, Holowka and Webb, which used these vesicles for characterization of plasma membrane lipid composition[10] and physical properties[11], domain formation[12] and the structural/biochemical properties of the IgE receptor[13]. More recently, these vesicles have been used as cell membrane models to test the membrane permeability of various molecules for drug delivery applications[14,15].

Phase separation in GPMVs

The original observation of phase separation in GPMVs also contained the critical observation that membrane components, including both proteins and lipids, were sorted preferentially into one or the other of the coexisting phases[6], often according to predictions from biochemical raft preparations (i.e., detergent resistance)[16]. Because of this enrichment of many putative raft components in the more ordered phase of GPMVs, this phase is often referred to (and will be referred to here) as the 'raft phase'. However, this terminology should not be taken as an indication of equivalence between the raft phase in GPMVs and the nanoscale, dynamic rafts postulated in live cells—not least because GPMVs are at thermodynamic equilibrium, a situation clearly not reflective of biology (see 'Limitations of GPMVs' below). Furthering the analogy between the raft phase in GPMVs and biochemical raft preparations, there was a qualitative correlation between both the temperature and cholesterol dependence of detergent resistance and phase separation[17]. These studies were followed up by partitioning experiments to define the structural determinants of lipid and protein partitioning to the raft phase. For lipids, the general paradigm of

a sphingosine backbone and longer, more saturated acyl chains being raftophilic seems to be applicable; however, marked perturbations can be induced by the polar head group and addition of a bulky fluorescent tracer[16,18]. Although proteins anchored to the membrane by a glycophosphatidylinositol (GPI) anchor (usually containing two saturated acyl chains) were consistently enriched in the raft phase[16,19], most transmembrane proteins require post-translational modification by a saturated fatty acid (palmitoylation) for raft phase partitioning[19]. As noted below, palmitoylation is sensitive to the preparation conditions, possibly explaining the lack of correlation between raft phase partitioning and detergent resistance of several transmembrane proteins[20]. Finally, the remarkable observation of critical behavior in GPMVs provides a possible link between the microscopic phase segregation observed at non-physiological conditions (i.e., low temperature, isolated membrane), and the nanoscopic organization present in live cells[21].

Alternative techniques

Before the development of GPMVs, the standard and nearly exclusive criterion for assigning raft association was insolubility in cold (4 °C) nonionic detergents[22]. Such preparations clearly do not reflect the organization of an unsolubilized membrane at physiological temperature and tend to be highly variable because of the complex molecular interactions between detergents and membrane components. Finally, different detergents yield insoluble fractions of different compositions[23,24], demonstrating that detergent-resistance alone is an inadequate, or at least incomplete, method for defining raft composition.

Giant unilamellar vesicles (GUVs) synthesized from pure lipid components show liquid-liquid phase coexistence due to the preferential association of sterols with saturated lipids, especially sphingolipids, to form the liquid-ordered (L_o) phase, which is immiscible with the unsaturated lipid-rich liquid-disordered (L_d) phase[25–27]. This collective segregation has been the primary 'minimal' model of raft separation in eukaryotic membranes and has helped to elucidate the physicochemical principles and molecular interactions behind raft formation; however, the biological relevance of such model systems is inherently limited by their compositional simplicity and (typically) lack of integral membrane proteins (for comparison between GUVs and GPMVs, see **Table 1**).

Finally, a recently developed technique, plasma membrane spheres, allows swelling of the plasma membranes away from the rest of the cellular components—large-scale separation of the membrane can be then induced by cross-linking of raft glycosphingolipids[7]. Although this method includes many of the advantages of GPMVs, it is somewhat limited because only certain cell types show the swelling behavior required to form plasma membrane spheres and these must contain enough GM1 glycolipid such that cross-linking induces raft coalescence.

Limitations of GPMVs as a plasma membrane model system

The obvious and most notable limitations of GPMVs are the covalent modifications induced by chemical vesiculants. The more common preparation involves a combination of formaldehyde and dithiothreitol, which are nonspecific cross-linkers and reducers, respectively. Adaptations of this protocol[19,28] have circumvented these undesirable side-effects by *N*-ethyl maleimide (NEM), which irreversibly reacts with terminal sulfhydryls (typically cysteine side chains), covalently blocking these groups without cross-linking. Beyond the simple chemical modifications required for vesicle formation, there is a myriad of possible cellular events that occur during the vesicle isolation procedure—because these are so complex and nearly impossible to predict, these comprise the broadest limitation of GPMVs. A known example is the loss of membrane leaflet asymmetry, typically defined by the exposure of the anionic lipid phosphatidylserine. Although GPMV membranes are asymmetric to some degree (e.g., proteins likely retain their native topology), phosphatidylserine is clearly exposed on the exoplasmic leaflet[6], in contrast to live cell plasma membranes. The mechanism (i.e., active scrambling or passive lipid flipping) and extent of loss of bilayer asymmetry is not known, nor is the effect of scrambling on phase separation. Similarly, the potential of lipid- and protein-modifying enzymes and/or membrane trafficking to affect membrane composition is clearly not negligible (e.g., PIP2 appears to be depleted[29]), and cannot be ruled out. Finally, GPMVs represent the cellular membrane in a state of thermodynamic equilibrium, whereas the live cell membrane is a highly dynamic and out-of-equilibrium environment whose composition is constantly modified by vesicle trafficking, enzyme activity, interaction with cytoskeletal components and so on. Therefore, GPMVs can be indicative, but not definitive, about raft organization or domain preference of a given molecule in the living cell.

Despite these limitations, the protocol described here[6,16,17,19,28] is a simple way to produce microscopic plasma membrane vesicles where phase separation can be easily visualized, the order of the coexisting phases can be measured and component partitioning between coexisting domains can be directly and quantitatively evaluated. Because of this simplicity, this model system provides an essential ingredient of the general toolbox for research into membrane organization, and a way forward for investigation of raft-dependent phenomena.

TABLE 1 | Comparing properties of GUVs and GPMVs.

Characteristic	GUV	GPMV
Complexity	Simple lipid composition; few, if any, proteins reconstituted	Physiological lipid complexity, contains native proteins[8,10]
Order difference between phases	Large (>1.0 GP units)[37]	Small (~0.2 GP units)[37]
Protein partitioning	Most peptides/proteins enrich in disordered phase[38–40]	GPI-anchored and some palmitoylated proteins are raft phase preferring[6,16,19]
Lipid analog partitioning	Most lipid analogs are disordered phase preferring[41]	Many lipid analogs retain partitioning characteristics of native lipids[18]
Diffusivity difference between phases	$D_{L_d}/D_{L_o} \cong 10$ (ref. 42)	$D_{L_d}/D_{L_o} \cong 3$ (ref. 17)
Microscopic phase separation temperature	Up to 35–38 °C (ref. 25)	Preparation-dependent; below 20 °C (ref. 28)

GUV standard raft mixture; dioleoylphosphatidylcholine:sphingomyelin:cholesterol at 2:2:1.
D, diffusion coefficient.

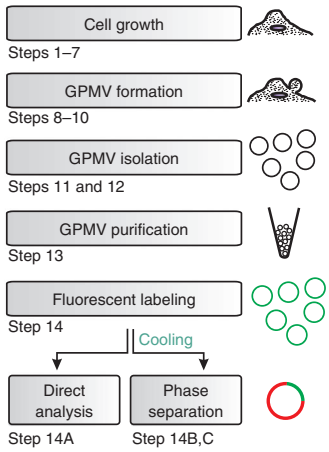

Figure 1 | Overview of the protocol. Giant plasma membrane vesicles can be isolated from a variety of cell types by addition of vesiculation chemicals followed by separation of vesicles from attached cells. These GPMVs can then be used for fluorescence imaging of proteins and/or membrane domains. Green circles represent fluorescently labeled vesicles, whereas those with red and green areas represent phase-seperated GPMVs.

Experimental design

GPMVs can be isolated from a variety of mammalian cell types; however, adherent cells generally provide better yields and purities because these cells remain attached to the dish during vesiculation while the vesicles themselves are released into the supernatant. The basic protocol for preparing GPMVs is simple—cells are treated with [Ca^{2+}]-containing buffer supplemented with vesiculation agents at 37 °C. GPMV formation then proceeds over the course of ~1 h (**Supplementary Video 1**). A graphical overview of the complete protocol is depicted in **Figure 1**.

Purification and concentration of membranes. After formation, GPMVs can be separated from adherent cells by transferring the supernatant by pipette. Although most cells remain attached to the plate (**Fig. 2**), cellular debris in the supernatant can be separated from GPMVs by differential centrifugation—cell debris pellets almost completely at ~100*g*, whereas vesicles can be collected by centrifugal forces of ≥20,000*g* (ref. 30). This procedure results in the recovery of ~20% of original plasma membrane material[30]. These steps are only necessary if the membrane material is used for biochemical experiments where purity is an important concern—for microscopy, GPMVs can be easily distinguished from cellular debris, thus obviating the need for purification. Vesicles can be concentrated for microscopy by allowing them to sediment at 4 °C and then removing the supernatant or pipetting the sample directly from the bottom of the container.

For biochemistry, lipid and protein concentrations can be measured by standard methods (e.g., Bradford or phosphate assay). In addition, the relative concentration of membranes in GPMV suspensions can be estimated by spectroscopy. The emission spectrum (λ_{ex} = 385 nm) of unlabeled bilayer membranes typically has a relatively strong emission peak at 425 nm (**Fig. 3a**)—the intensity of this peak correlates well with the amount of membrane in the sample, as judged by standard biochemical assays[31]. As background fluorescence above 450 nm is independent of the sample concentration, the relative intensity of the peak at 425 nm can be used to normalize sample membrane concentrations[31].

Considerations for visualization of GPMVs by fluorescence microscopy. GPMVs can be visualized by bright-field microscopy because of the refractive index difference between the cytoplasm inside the GPMVs and the buffer outside (**Fig. 2a**,**b**). Alternatively, GPMVs can be imaged using fluorescence microscopy (**Fig. 2c**) by one of three methods: (i) labeling cellular plasma membranes with fluorescent markers before vesicle isolation; (ii) direct labeling of isolated vesicles; or (iii) transfection of cells with fluorescent chimeras of plasma membrane proteins. Each method has distinct advantages. Direct labeling of isolated vesicles is the simplest method—addition of lipophilic dyes directly to vesicle suspensions leads to rapid incorporation into membranes. The drawback of this approach is high background fluorescence from unincorporated dye and, more importantly, poor control of relative fluorescent analog loading. This drawback is important because high levels of fluorescent lipid analogs would be expected to affect the biophysical properties of the membranes. In addition, it is important to be aware of potential artifacts induced by photooxidation of fluorescent dyes, which has been shown to affect phase separation[32]. Labeling cells before isolation yields more uniform labeling with less background fluorescence, but requires more dye and several preisolation labeling steps. Finally, expression of fluorescent proteins offers the least perturbing approach to visualizing the membrane (since the fluorescent moiety is typically far away from the membrane portion of the protein), but yields much lower fluorescent signal because of the limited expression and transfection efficiency.

Quantification of phase order in GPMVs. A potential application for GPMVs is the quantification of the physicochemical properties of isolated plasma membranes and/or relative differences between the coexisting raft and nonraft phases. A key property defining the state of membranes is the conformational order of the acyl chains in the hydrophobic core of the bilayer. This order can be explicitly measured in pure lipid systems by NMR; in biological membranes, a simple approach to approximate the relative order/lipid packing of membranes is the use of polarity-sensitive dyes, the most widely used being laurdan. This fluorescent lipid shows a water-induced emission shift between the relatively ordered (tightly packed, less aqueous) phase where the emission peak is at 440 nm and the relatively disordered (loosely packed, more aqueous) phase with maximal emission at 490 nm (**Fig. 3b**). A normalized polarity index, generalized polarization (GP), is used to express the relative emission shift, reflective of membrane packing/order:

$$GP = \frac{\sum_{420}^{460} I_x - \sum_{470}^{510} I_x}{\sum_{420}^{460} I_x + \sum_{470}^{510} I_x} \quad (1)$$

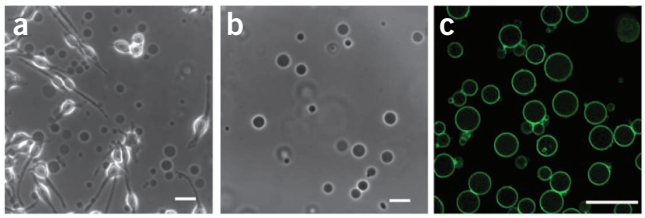

Figure 2 | GPMV visualization. (**a**,**b**) GPMVs are observable by bright-field microscopy either in the presence of cells (**a**) or after isolation (**b**). (**c**) GPMVs can be observed by fluorescence microscopy after labeling the membranes with a fluorescent amphiphilic dye (FAST-DiO). Scale bars, 20 μm.

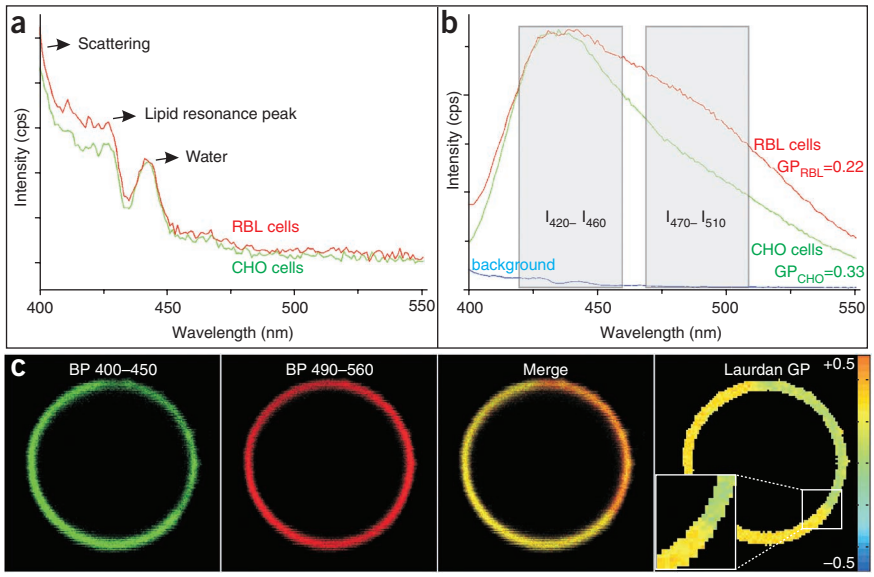

Figure 3 | C-laurdan characterization of GPMVs. (**a**) The membrane concentration of GPMV suspensions can be normalized by spectroscopy of unstained membranes. Upon excitation at 385 nm, GPMV suspensions give a characteristic scattering spectrum with a water Raman scattering peak at 440 nm and a lipid scattering peak at 425 nm. This lipid peak is directly proportional to the membrane concentration of the sample and can be used to normalize across samples/preparation conditions[31]. Shown are emission spectra from unstained GPMVs isolated from two common cell culture lines, rat basophilic leukemia (RBL; red) and Chinese hamster ovary (CHO; green) cells. (**b**) Lipid packing/order can be quantified by fluorescence spectroscopy of an environment-sensitive fluorophore (C-laurdan). Shown are the C-laurdan emission spectra of GPMVs isolated from cell culture lines shown in **a**. The different degree of spectral red shift (i.e., the higher emission intensities of RBL GPMVs between 470 and 510 nm) indicates that GPMVs from RBL cells are less ordered than those from CHO cells. Wavelength ranges used to calculate generalized polarization (GP) by equation (1) are shown as gray boxes. (**c**) The order of coexisting phases in phase-separated GPMVs can be quantified using two-photon microscopy of the same dye by filtering emission light to select wavelengths representative of ordered (green) and disordered (red) phase emission. These can then be processed[33] to yield maps of the GP, a relative index of membrane order (right). c.p.s., counts per second.

In GPMVs with coexisting fluid phases, microscopy of laurdan can be used to simultaneously measure the order of both phases by splitting the fluorescence emission signal with band-pass filters selective for the ordered and disordered phase emissions (**Fig. 3c**). These images can then be processed to generate order maps, using correction factors to enforce agreement between micro- and spectroscopic data, as described[33].

Temperature-controlled imaging. The most important advantage of GPMVs compared with both pure lipid model systems and live cells is the ability to investigate microscopic phase separation in a membrane reflective of the true composition of biological plasma membranes. This phase behavior is inherently temperature-dependent, and thus it is often necessary to cool the system well below room temperature to observe phase separation in GPMVs. This requirement presents an experimental challenge, because most commercial temperature-controlled imaging systems are designed for warming samples to physiological temperatures, rather than cooling. Several different strategies have been implemented for accurate and rapid control of sample temperature (**Fig. 4**). All involve the construction of a sealed chamber consisting of two coverslips separated by a water-repellant sealant (e.g., paraffin wax) and containing the GPMV suspension (**Fig. 4a**). This chamber is typically imaged using an inverted microscope, because the vesicles quickly sink to the bottom of the chamber. In one construction, this chamber is attached directly to the underside of a metallic thermal insert, thus ensuring tight thermal coupling between the temperature controller and the sample (**Fig. 4b**). In this arrangement, the objective needs to be either thermally isolated from the sample (i.e., air-immersion objective) or if a fluid-immersion objective is desired for higher resolution, it should be cooled to the sample temperature to avoid heat flow and resulting temperature gradients which lead to convective flow. Another option to simultaneously cool the objective and sample is to immerse both in a water-filled chamber cooled by submerged coils[34].

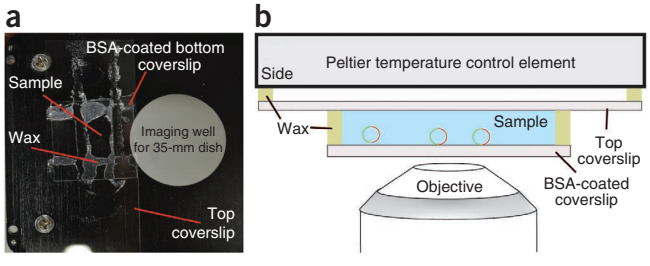

Characterization of component partitioning. One of the most notable uses of GPMVs is determination of lipid and protein partitioning between raft and nonraft phases[19,20,35], thereby providing a simple and quantitative method for estimating raft association. The method involves imaging the fluorescently labeled protein or lipid component concurrently with a reference marker with well-characterized phase partitioning (**Fig. 5a,b**). By using a reference marker for either phase, the relative concentration of the component of interest can then be quantified in both phases by a fluorescence intensity line scan through the two phases (white arrow in **Fig. 5b**). Raft phase partitioning can then be expressed as an equilibrium partition coefficient ($K_{p,raft} = I_{raft} / I_{nonraft}$) or as the percentage of protein in the raft phase (% raft = $I_{raft} / (I_{raft} + I_{nonraft})$) (**Fig. 5c**).

Controls. Counterstaining of apposing phases with different fluorescent markers (**Fig. 5a**) is an important control for the presence of coexisting selective phases. Appropriate markers for the raft phase

Figure 4 | Temperature-controlled imaging. To observe phase separation in GPMVs, it is often necessary to cool the sample. A useful construction involves a small volume (10–25 µl) of sample between two coverslips separated by wax sealant. (**a**,**b**) Shown is a photograph (**a**) and a schematic image of this chamber mounted directly on a thermal insert (**b**). The imaging chamber is not placed in the well designed for imaging (gray circle in **a**), but rather attached directly to the underside of the cooled microscope stage (black surface in **a**).

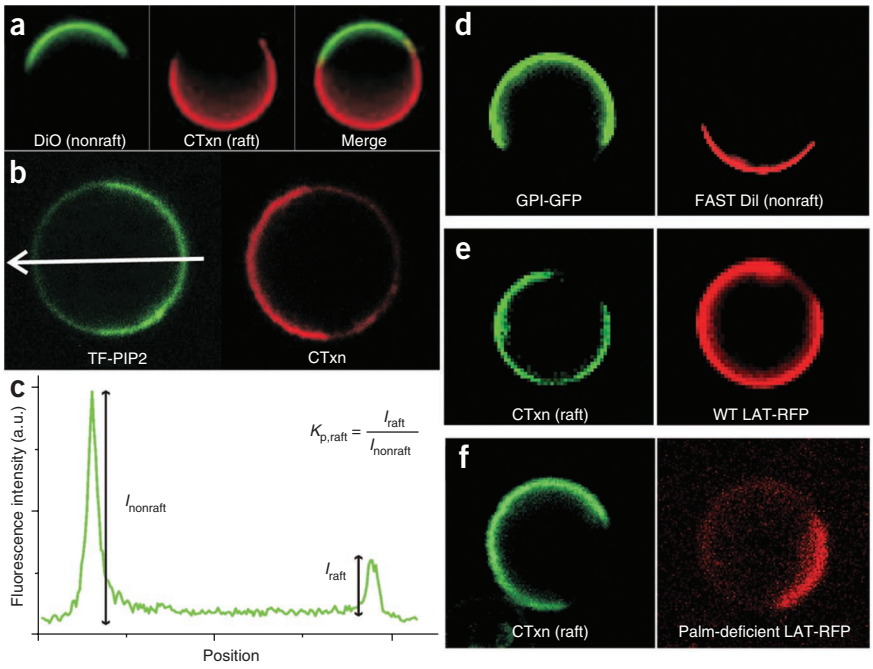

Figure 5 | Quantification of component partitioning. (**a**) Phase identity in separated GPMVs can be confirmed by well-characterized markers. Unsaturated lipidic dyes (e.g., FAST-DiO—left) and glycosphingolipid-binding proteins (CTxn; e.g., the B-subunit of cholera toxin—middle) are bona fide markers of the nonraft and raft phases, respectively. (**b**,**c**) The partitioning of a component of interest (**b**) (TopFluor (TF)-PIP2; left; white arrow represents the line used for the intensity scan in part (**c**)) between the coexisting phases identified by a well-established marker (right) can be quantified by a fluorescence intensity line scan through the two phases (**c**). The ratio of fluorescence in the raft and nonraft phase gives a quantitative measurement ($K_{p,raft}$) of phase preference. (**d**–**f**) The partitioning of some well-characterized membrane proteins in NEM GPMVs is shown: GPI-anchored GFP (**d**) and the doubly palmitoylated transmembrane linker for activation of T-cells (LAT) (**e**) are strongly enriched in the raft phase. (**f**) The palmitoylation deficient mutant of LAT (LAT-C26A) is depleted from the raft phase. For experimental details, see ref. 19. a.u., arbitrary units.

are the B subunit of cholera toxin (binds the raft glycolipid GM1), some cholesterol analogs (e.g., Bodipy-cholesterol), napthopyrene, and/or GPI-anchored proteins, whereas nonraft phases are typically marked by unsaturated lipid analogs. **Figure 5d–f** shows the partitioning of various proteins that could be used as controls for phase separation and appropriate partitioning.

MATERIALS

REAGENTS

- Cells (rat basophilic leukemia (RBL); American Type Culture Collection)
- Cell culture medium, MEM (Invitrogen, cat. no. 21090-022)
- Paraformaldehyde (PFA; Sigma-Aldrich, cat. no. 16005) **! CAUTION** PFA is a suspected carcinogen. Use gloves and avoid contact.
- Dithiothreitol (DTT; Sigma-Aldrich, cat. no. D0632) **! CAUTION** DTT is toxic. Use gloves and avoid contact.
- NEM (Sigma-Aldrich, cat. no. E3876) **! CAUTION** NEM is toxic. Use gloves and avoid contact.
- 3,3′-Dilinoleyloxacarbocyanine perchlorate (FAST-DiO; Invitrogen, cat. no. D3898)
- 1,1′-Dilinoleyl-3,3,3′,3′-tetramethylindocarbocyanine, 4-chlorobenzenesulfonate (FAST-DiI; Invitrogen, cat. no. D7756)
- 1-Oleoyl-2-{6-[4-(dipyrromethene boron difluoride)butanoyl]amino}hexanoyl-*sn*-glycero-3-phosphoinositol-4,5 bisphosphate (TopFluor-PIP2; Avanti Polar Lipids, cat. no. 810184)
- Cholera toxin B subunit with desired fluorescent tag (CTxB; Invitrogen, cat. nos. C-34775, C-34776, C-34777, C-34778)
- Laurdan (Molecular Probes, cat. no. D250) or C-laurdan[36]
- Sodium chloride (NaCl; Sigma-Aldrich, cat. no. S7653)
- Potassium chloride (KCl; Sigma-Aldrich, cat. no. P9333)
- Calcium chloride ($CaCl_2$; Sigma-Aldrich, cat. no. C1016)
- HEPES (Sigma-Aldrich, cat. no. H3375)
- Potassium phosphate monobasic (KH_2PO_4; Sigma-Aldrich, cat. no. P5655)
- Sodium phosphate dibasic heptahydrate ($Na_2HPO_4 \bullet 7H_2O$; Sigma-Aldrich, cat. no. 431478)
- Hydrochloric acid (HCl; Sigma-Aldrich, cat. no. H1758)
- Sodium hydroxide (NaOH; Sigma-Aldrich, S8045)
- Bovine serum albumin (BSA; Sigma-Aldrich, A7906)
- Paraffin wax (Sigma-Aldrich, cat. no. 327204)
- Vesiculation agents in GPMV buffer (PFA/DTT, NEM; see REAGENT SETUP)
- Ethanol
- Distilled H_2O

EQUIPMENT

- 37 °C Incubator
- Microcentrifuge tubes (Eppendorf)
- Coverslips (no. 1.5; 22 × 22 mm and 24 × 60 mm) or Labtek chambers or MatTek chambers
- Spectrofluorimeter
- Spectroscopy cuvette
- Confocal microscope (e.g., Zeiss LSM 510 or comparable)
- Two-photon microscope including appropriate dichroic mirror, filters and λ/4 plate
- Temperature controller fitted for MatTek and/or LabTek chambers (Warner Instruments; cat. no. 64-0352)
- Thermal inserts for MatTek and/or LabTek chambers (Warner Instruments, cat. nos. 64-1636, 64-1646)
- Objective cooling ring (Bioptechs, cat. no. 150303)
- ×40 air- or water-immersion objective
- Circulating water bath with 8-mm hoses

REAGENT SETUP

PBS To prepare PBS (137 mM NaCl, 2.7 mM KCl, 10 mM $Na_2HPO_4 \bullet 2H_2O$, 2 mM KH_2PO_4, pH 7.4), dissolve 8 g of NaCl, 0.2 g of KCl, 1.78 g of $Na_2HPO_4 \bullet 2H_2O$ and 0.27 g of KH_2PO_4 in distilled water and bring to 1 liter. Adjust the pH with HCl or NaOH to 7.4. This can be stored for 1 year at room temperature (23 °C).

GPMV buffer To prepare GPMV buffer (10 mM HEPES, 150 mM NaCl, 2 mM $CaCl_2$, pH7.4), dissolve 8.75 g of NaCl, 0.22 g of $CaCl_2$ and 2.38 g of HEPES in distilled water and bring to 1 liter. Adjust the pH with HCl or NaOH to 7.4. This can be stored at room temperature or at 4 °C for 6 months.

FAST-DiO and FAST-DiI solutions The solid dyes are dissolved in ethanol. The stock solutions are optimally 0.5 mg ml^{-1}. Stock solutions can be kept for 1 year at −20 °C. A dilution of 1:100 is convenient for the experiments. The stocks should be kept in lightproof vials.

PFA solution (4% (wt/vol)) Dissolve 4 g of PFA in 50 ml of distilled H_2O. Heat to above 50 °C and adjust the pH with HCl/NaOH until the solution clears. Bring the final volume to 100 ml. The stock can be stored at 4 °C for 1 year.

DTT solution (1 M) Dissolve 1.54 g DTT in distilled H_2O and bring the volume to 10 ml. The stock can be stored at −20 °C for 1 year.
NEM solution (1 M) Dissolve 1.25 g NEM in distilled H_2O and bring the volume to 10 ml. The stock can be stored at −20 °C for 3–6 months. It should not be used when the solution starts to turn yellow.
PFA/DTT To prepare 25 mM PFA/2 mM DTT, add 18 µl of 4% (wt/vol) PFA solution and 2 µl of 1 M DTT solution to 1 ml of GPMV buffer. The solution should be freshly prepared.
NEM (2 mM) Add 2 µl of 1 M NEM to 1 ml of GPMV buffer. The solution should be freshly prepared.
BSA solution (1 mg ml^{-1}) Dissolve 50 mg of BSA in distilled water and bring the volume to 50 ml. The stock can be stored at 4 °C for 1 year.

EQUIPMENT SETUP

Preparation of BSA-coated coverslips and chambers Incubate coverslips in 1 mg ml^{-1} BSA solution for 1 h. For LabTek chambers, add 250 µl of 1 mg ml^{-1} BSA solution into the wells and incubate for 1 h. Wash two times with PBS. The coating should be done immediately before use.
Imaging chamber construction Put the wax sealant on the top coverslip (24 × 60 mm) in a square shape (approximately 15 × 15 mm). Pipette 10–15 µl of GPMV suspension into the middle of the square. Place a BSA-coated coverslip (22 × 22 mm^2) on the wax sealant square and turn the chamber upside down so that the BSA-coated coverslip is the bottom of the chamber. A small spot of wax sealant on the top side of the top coverslip can then be used to attach the imaging chamber to the cooled microscope stage/insert.
Cooling system Connect the thermal inserts and objective cooler to a circulating, temperature-controlled water bath with rubber hoses. The hoses should be sealed at the connection points. The water bath temperature should be approximately equal to the desired chamber/sample temperature. **! CAUTION** If you are using a Peltier-element temperature controller, water circulation should begin before temperature regulation in order to remove the heat produced in the device. **! CAUTION** If objective cooling is necessary to avoid heat flow to the sample, care must be taken to thermally isolate the objective from the rest of the microscope to avoid condensation inside the microscope box. **▲ CRITICAL** If the cooling setup in **Figure 4b** is used with an air-immersion objective, cooling the objective is unnecessary. However, condensation can form on the sample surface, hindering imaging. To avoid this, a stream of dehumidified air or N_2 can be blown directly in the space between the objective and sample.
Confocal microscopy The optical configuration should be set according to the dyes used. The lasers should be switched on at least 15 min before the measurements. If fluorescent lipid components with dipoles oriented relative to the plane of the membrane (most lipidic dyes) are used, a λ/4 plate is required to depolarize the excitation laser light and ensure uniform excitation. For fluorescent protein chimeras, this is typically unnecessary because the proteinaceous fluorophores are well removed from the membrane and their orientation is unlikely to be considerably constrained.
Two-photon setup Excitation of laurdan dyes requires wavelengths (~400 nm) that are unavailable on most standard confocal microscopes and induce substantial photobleaching; thus, two-photon excitation with 800-nm light is often used. The emission signal should be split by a dichroic mirror with a cutoff of ~465 nm and further filtered for ordered channel (430/30 nm or similar) and disordered channel (500/30 nm or similar) emission. Laurdan's excitation dipole orients perpendicular to the plane of the membrane, thus polarized light excitation will lead to nonuniform excitation of laurdan molecules and the appearance of heterogeneity. A λ/4 plate is required to depolarize the excitation laser light and ensure uniform excitation. Images are best taken at the equatorial plane of the vesicle as there may be artifacts while imaging at the vesicle poles because of photoselectivity. Details for GP calculations from such images are given in extensive protocols by Owen *et al.*[33] and Kaiser *et al.*[37].

PROCEDURE

Preparation of cells ● TIMING time required to reach 70% confluency (1–2 d)

1| Seed the cells in an appropriate chamber.
▲ CRITICAL STEP This protocol is optimized for cells seeded in 35-mm cell culture dishes. Refer to **Box 1** for the approximate cell numbers necessary for various experiments.
▲ CRITICAL STEP Seed the cells on a no. 1.5 glass slide (or MatTek/LabTek chamber) if imaging or spectroscopy of cell-attached GPMVs is needed.

2| Incubate the chambers in appropriate conditions until cells reach ~70% confluency. Check the American Type Culture Collection database (http://www.atcc.org/) for the appropriate conditions and media.

3| (Optional) Manipulate the cell culture (e.g., transfection) depending on the experiment. If quantification of protein partitioning is desired (see Step 14C), fluorescently tagged proteins should be transfected into cells before vesicle isolation.
▲ CRITICAL STEP Many common transfection agents are based on complexing DNA with cationic lipids. Such reagents should be avoided, particularly for biophysical experiments on isolated membranes, because of unknown effects of these exogenous lipids on plasma membrane structure/composition.

Box 1 | Tips for GPMV yield

The vesicle yield correlates directly with the number of cells used for the preparation; thus, the maximal density of cells that are compatible with the experiment should be used. For microscopic experiments, a 35-mm dish of cells at 70% confluence should be sufficient for a number of individual samples. For biochemistry, e.g., western blotting, it is often necessary to start with a 10-cm dish. GPMV formation is a function of incubation temperature—at 37 °C, blebbing is completed within 1 h. Colder temperatures, e.g., room temperature or even 4 °C, still allow vesicle formation, but require longer incubation times (overnight for 4 °C). Shaking the cell plates during GMPV preparation can increase vesicle yield, but this comes at the cost of decreased purity, as more whole cells will detach from the dish. Finally, the concentrations of the vesiculation chemicals can be varied by an order of magnitude in both directions while still allowing GPMV formation[28]. These parameters (chemical concentration, incubation time, incubation temperature, shaking) should be optimized for each specific cell type, although the conditions described here have proven successful for a number of different cultured cell lines.

Labeling cell membranes before GMPV isolation ● **TIMING 30 min**

▲ **CRITICAL** This section is optional; if post-isolation labeling is desired, skip these steps and go directly to Step 8.

4| Wash the cells two times with 1 ml PBS.

5| Add 10 µl of dye solution to 1 ml of PBS (final concentration = 5 µg/ml) and add it to the cells.

6| Incubate at 4 °C for 10 min to allow dye incorporation into membranes.

▲ **CRITICAL STEP** Concentrations and incorporation conditions should be optimized for all dyes, although the above conditions give good results for the dialkylcarbocyanine (i.e., DiO, DiI and so on) dyes used here.

7| Aspirate the dye solution, wash five times with PBS to remove unincorporated dye, and proceed to GPMV isolation (Step 8).

Isolation of GPMVs ● **TIMING 2 h**

8| Wash cells twice with 1 ml of GPMV buffer (see REAGENT SETUP).

9| Add 1 ml of buffer containing vesiculation agents in GPMV buffer (see MATERIALS) to cells.

▲ **CRITICAL STEP** PFA causes cross-linking of proteins and DTT cleaves thioester bonds. For the problems these phenomena can create and a comparison between PFA/DTT and NEM preparations, see **Box 2**.

10| Incubate the cells at 37 °C for 1 h.

11| Remove the chambers from the incubator and check for the presence of vesicles. These should be readily observable at ×20 magnification as dark free-floating spheres at the plane of the cells (**Fig. 2**). For tips on GPMV yield, see **Box 1**.

? TROUBLESHOOTING

12| Transfer the GPMV-rich cellular supernatant into a microcentrifuge tube by pipetting.

■ **PAUSE POINT** After isolation, GPMVs can be stored at 4 °C for 1–2 d without visible degradation.

13| To concentrate the GPMV suspension for biochemical or spectroscopic experiments where vesicle morphology is irrelevant, centrifuge the GPMV suspension at 100*g* for 10 min to pellet cell debris, then again at 20,000*g* for 1 h at 4 °C to pellet GPMV membranes (this should be done for laurdan spectroscopy to measure membrane order, Step 14A). Alternatively, for imaging experiments in which purity is not important (laurdan microscopy to visualize membrane order, Step 14B, and confocal microscopy to measure component partitioning, Step 14C), leave the GPMV suspension in the microcentrifuge tube for 20–30 min; GPMVs will concentrate at the bottom of the tube.

Analysis of isolated GPMVs

14| Use option A to measure the membrane order with laurdan spectroscopy, option B to visualize the membrane order by laurdan microscopy or option C to measure component partitioning with confocal microscopy.

(A) Laurdan spectroscopy of GPMVs ● **TIMING 2 h**

(i) Discard the supernatant from Step 13 and resuspend the pellet in ~60 µl of GPMV buffer by gentle pipetting.

▲ **CRITICAL STEP** Be careful not to disrupt the membrane pellet while discarding the supernatant.

(ii) Transfer the GPMV suspension to a spectroscopy cuvette.

▲ **CRITICAL STEP** Performing Step 14A(iii–v) to equalize the membrane amount according to the 425-nm lipid peak

Box 2 | Artifacts induced by vesiculation chemicals

The most efficient, cleanest, and therefore most common preparation for GPMVs involves the mixture of 25 mM formaldehyde and 2 mM DTT as the vesiculants. Unfortunately, this preparation induces several unwanted artifacts: (i) nonspecific cross-linking of lipids and proteins by the aldehyde, which precludes many types of protein analysis (e.g., PAGE); (ii) cleavage of protein disulfides and thioesters, leading to depalmitoylation[19]; (iii) specific coupling of phosphatidylethanolamines to proteins[28]. This last effect seems to have the biggest impact on phase behavior/properties in the GPMVs, increasing the miscibility transition temperature (i.e., the highest temperature at which coexisting domains are observable) by ~15 °C. To avoid many of these artifacts, non-cross-linking vesiculants like *N*-ethyl maleimide are suggested; however, these present experimental challenges because they require cooling the sample to below 5 °C to observe microscopic phase coexistence. Other chemicals that cross the plasma membrane and covalently block free sulfhydryls have been used for GPMV preparation[9]; their effects on phase behavior have not been measured.

and labeling of GPMVs with laurdan/C-laurdan are necessary only if the cells are not labeled before GPMV preparation (as described in Steps 4–7). If the cells are already labeled, skip Step 14A(iii–v) and proceed directly to Step 14A(vi).

(iii) Measure the emission spectrum from 400 to 550 nm with excitation at 385 nm.

(iv) Equalize the membrane concentration between various samples by diluting samples with GPMV buffer until 425-nm peaks are of approximately equal intensity (**Fig. 3a**). Use the sample with the lowest peak at 425 nm as the reference sample and dilute the other samples by the ratio of the reference sample 425-nm peak intensity to their 425-nm peak intensity. Repeat measurements of emission spectra to ensure approximate equality of 425-nm peaks.
▲ **CRITICAL STEP** The lipid scattering peak should be at least as intense as the Raman scattering peak of water observable at 440 nm (**Fig. 3a**), as this ensures a minimal amount of membrane for accurate spectroscopic analysis.
? TROUBLESHOOTING

(v) Add 3 µl of 8 µM C-laurdan solution to 57 µl of GPMV suspension (membrane concentration normalized as above; final [C-laurdan] = 0.4 µM).
▲ **CRITICAL STEP** C-laurdan is recommended for GPMV and cell experiments that require incorporation into preassembled membranes.
▲ **CRITICAL STEP** High dye concentrations may affect the physical properties of membranes, and thus these should always be kept to the minimal concentrations that give adequate signal-to-noise ratios.
■ **PAUSE POINT** Incubate for 30 min for efficient staining.

(vi) Excite sample with 385-nm light and measure fluorescence from 400 to 550 nm (**Fig. 3b**).

(vii) Calculate GP as shown in equation (1).

(B) Laurdan microscopy of GPMVs ● TIMING 2 h

(i) Pipette 50 µl of GPMV suspension from the bottom of the tube from Step 13 for labeling.

(ii) Add 1 µl of 0.2 mM laurdan/C-laurdan solution to a concentrated GPMV suspension and allow at least 30 min for dye incorporation.
▲ **CRITICAL STEP** This step is only necessary if cell membranes were not already labeled in Steps 4–7.

(iii) Construct an imaging chamber as shown in **Figure 4** and let the temperature equilibrate for at least 10 min. This time will also allow the vesicles to sink to the bottom of the chamber.
▲ **CRITICAL STEP** The bottom coverslip of the imaging chambers should be coated with BSA to avoid nonspecific sticking/bursting of the GPMVs on the glass.

(iv) Before imaging, decrease the temperature of the sample below 15 °C for GPMVs derived with PFA/DTT and below 5 °C for NEM GPMVs (**Box 2**).
▲ **CRITICAL STEP** If immersion objectives are used, they must also be cooled to avoid heating of the sample by the objective (see EQUIPMENT SETUP). If air objectives are used, condensation at the bottom of the coverslip can be avoided by air or nitrogen flow directly onto the coverslip.

(v) Excite the dye with 800-nm laser light in the two-photon setup and record emission separately from disordered and ordered channels (centered around 440 and 490 nm, respectively).
▲ **CRITICAL STEP** Image vesicles at the equatorial plane and use a $\lambda/4$ plate to ensure the uniform excitation (see EQUIPMENT SETUP).
? TROUBLESHOOTING

(vi) Calculate the GP with appropriate corrections for microscope settings as described[33] (**Fig. 3c**).

(C) Confocal imaging of GPMVs and quantification of partitioning ● TIMING 2 h

(i) Follow Step 14B(i) to prepare GPMVs for labeling.

(ii) Add 0.5 µl of 0.5 mg ml^{-1} FAST-DiO or FAST-DiI to label the nonraft phase or the same amount of fluorescent CTxB to label the raft phase according to the desired optical setup. If quantification of protein partitioning is desired, fluorescently tagged proteins should be transfected into cells before vesicle isolation (see Step 3).
▲ **CRITICAL STEP** This step is only necessary if cell membranes were not already labeled in Steps 4–7.
▲ **CRITICAL STEP** Avoid high dye concentration.
▲ **CRITICAL STEP** Effective CTxB labeling is limited by the amount of GM1 in the cell membrane. Excess CTxB produces background.

(iii) Construct an imaging chamber as in Step 14B(iii).

(iv) Decrease the temperature below 15 °C for GPMVs derived with PFA/DTT and below 5 °C for the ones derived with NEM.

(v) Excite with the proper lasers and record emission.
▲ **CRITICAL STEP** One channel should always be used to image a well-characterized marker of either the raft or nonraft phase (e.g., unsaturated lipids for nonraft; cholera toxin for raft) while imaging the component of interest in the other (**Fig. 5a**,**b**).
▲ **CRITICAL STEP** Use lowest laser power possible to avoid photobleaching and oxidation.
? TROUBLESHOOTING

(vi) Quantify component partitioning from confocal microscopy images as shown in **Figure 5b**,**c**.
▲ **CRITICAL STEP** This calculation is only valid if the fluorescence quantum yield of the fluorophore in question is equal in the two coexisting phases. For fluorescent proteins, this is almost certainly the case, as they are well removed from the disparate lipid environments. The quantum yield of fluorescently labeled lipids may, however, be affected and this effect needs to be controlled for by separate experiments (see ref. 18).

? TROUBLESHOOTING

Troubleshooting advice can be found in **Table 2**.

TABLE 2 | Troubleshooting table.

Step	Problem	Possible reason	Solution
11	No vesicles; many detached cells	Vesiculation conditions are not appropriate for the cell type	Try different vesiculant chemicals or concentrations, and vary vesiculation time (see **Box 1**)
14A(iv)	No lipid peak at 425 nm	Low concentration of membrane	Increase vesicle yield with the steps in **Box 1** or increase the starting amount of cells
	Scattering curve does not look like **Figure 3a**	Non-bilayer membranes present	Be sure to avoid detergents or possibly micelle-forming components in the preparation
14B(v), 14C(v)	No observable phase separation	Temperature is too high	Lower the temperature of the chamber and/or ensure that there is no heat flux from the sample to the objective, stage and so on
	No fluorescence	Dye concentration is too low	Increase the dye concentration
14C(v)	No observable phase separation	Marker partitions equally between coexisting phases	Try a different marker

● TIMING

Steps 1–3, cell culture: 1–2 d
Steps 4–7, labeling membranes: 30 min
Steps 8–13, GPMV isolation: 2 h
Step 14A, laurdan spectroscopy of GPMVs: 2 h
Step 14B, laurdan microscopy of GPMVs: 2 h
Step 14C, fluorescent labeling and confocal imaging of partitioning: 2 h

ANTICIPATED RESULTS

Here we summarize the protocol for GPMV preparation and isolation, giving three distinct examples of their application using quantitative fluorescence spectroscopy/microscopy. GPMV preparation and isolation is experimentally trivial—treatment of cells with GPMV buffer supplemented with chemical vesiculants results in the rapid (within 1 h) formation of GPMVs, which can be observed in the cell culture chamber with a bright-field microscope (**Fig. 2a**,**b**). Fluorescence imaging is also possible by labeling of membranes with fluorescent probes before vesicle isolation, or by addition of fluorescent lipids or membrane-binding proteins to GPMV suspensions after isolation (**Fig. 2c**). These isolated plasma membranes can then be analyzed by quantitative microscopy or spectroscopy. Examples given include C-laurdan spectroscopy to compare the relative packing of GPMVs derived from two common cell culture models, C-laurdan microscopy to define the order/packing of coexisting phases (**Fig. 3**), and confocal microscopy to quantify partitioning of membrane components between coexisting phases (**Fig. 5**).

Note: Supplementary information is available in the online version of the paper.

ACKNOWLEDGMENTS The work was supported by the Max Planck Society; Humboldt Foundation Postdoctoral Fellowship, Technical University of Dresden; Deutsche Forschung Gemeinschaft (DFG) 'Schwerpunktprogramm1175' grant SI459/2-1, 'Transregio 83' grant TRR83 TP02; European Science Foundation 'LIPIDPROD' grant SI459/3-1; Bundesministerium für Bildung und Forschung 'ForMaT' grant 03FO1212; US National Institutes of Health grant R21AI073409; and the Klaus Tschira Foundation.

AUTHOR CONTRIBUTIONS E.S. and I.L. gathered the data; E.S. and H.J.K. designed the laurdan experiments; I.L. and T.B. designed GPMV isolation,

microscopy and partitioning protocols; and E.S., P.S., K.S. and I.L. wrote the manuscript.

COMPETING FINANCIAL INTERESTS The authors declare no competing financial interests.

Published online at http://www.nature.com/doi:10.1038/nprot.2012.059.
Reprints and permissions information is available online at http://www.nature.com/reprints/index.html.

1. Simons, K. & Ikonen, E. Functional rafts in cell membranes. *Nature* **387**, 569–572 (1997).
2. Lingwood, D. & Simons, K. Lipid rafts as a membrane-organizing principle. *Science* **327**, 46–50 (2010).
3. Brameshuber, M. *et al.* Imaging of mobile long-lived nanoplatforms in the live cell plasma membrane. *J. Biol. Chem.* **285**, 41765–41771 (2010).
4. Eggeling, C. *et al.* Direct observation of the nanoscale dynamics of membrane lipids in a living cell. *Nature* **457**, 1159–1162 (2009).
5. Gaus, K., Chklovskaia, E., Fazekas de St Groth, B., Jessup, W. & Harder, T. Condensation of the plasma membrane at the site of T lymphocyte activation. *J. Cell. Biol.* **171**, 121–131 (2005).
6. Baumgart, T. *et al.* Large-scale fluid/fluid phase separation of proteins and lipids in giant plasma membrane vesicles. *Proc. Natl. Acad. Sci. USA* **104**, 3165–3170 (2007).
7. Lingwood, D., Ries, J., Schwille, P. & Simons, K. Plasma membranes are poised for activation of raft phase coalescence at physiological temperature. *Proc. Natl. Acad. Sci. USA* **105**, 10005–10010 (2008).
8. Scott, R.E. Plasma membrane vesiculation: a new technique for isolation of plasma membranes. *Science* **194**, 743–745 (1976).
9. Scott, R.E., Perkins, R.G., Zschunke, M.A., Hoerl, B.J. & Maercklein, P.B. Plasma membrane vesiculation in 3T3 and SV3T3 cells. I. Morphological and biochemical characterization. *J. Cell Sci.* **35**, 229–243 (1979).
10. Fridriksson, E.K. *et al.* Quantitative analysis of phospholipids in functionally important membrane domains from RBL-2H3 mast cells using tandem high-resolution mass spectrometry. *Biochemistry* **38**, 8056–8063 (1999).
11. Tank, D.W., Wu, E.S. & Webb, W.W. Enhanced molecular diffusibility in muscle membrane blebs: release of lateral constraints. *J. Cell Biol.* **92**, 207–212 (1982).
12. Ge, M. *et al.* Ordered and disordered phases coexist in plasma membrane vesicles of RBL-2H3 mast cells. An ESR study. *Biophys. J.* **85**, 1278–1288 (2003).
13. Holowka, D. & Baird, B. Lactoperoxidase-catalyzed iodination of the receptor for immunoglobulin E at the cytoplasmic side of the plasma membrane. *J. Biol. Chem.* **259**, 3720–3728 (1984).
14. Dubavik, A. *et al.* Penetration of amphiphilic quantum dots through model and cellular plasma membranes. *ACS Nano* **6**, 2150–2156 (2012).
15. Saalik, P. *et al.* Penetration without cells: membrane translocation of cell-penetrating peptides in the model giant plasma membrane vesicles. *J. Control Release* **153**, 117–125 (2011).
16. Sengupta, P., Hammond, A., Holowka, D. & Baird, B. Structural determinants for partitioning of lipids and proteins between coexisting fluid phases in giant plasma membrane vesicles. *Biochim. Biophys. Acta* **1778**, 20–32 (2008).
17. Levental, I. *et al.* Cholesterol-dependent phase separation in cell-derived giant plasma-membrane vesicles. *Biochem. J.* **424**, 163–167 (2009).
18. Sezgin, E. *et al.* Partitioning, diffusion, and ligand binding of raft lipid analogs in model and cellular plasma membranes. *BBA—Biomembranes* published online, doi:10.1016/j.bbamem.2012.03.007 (17 March 2012).
19. Levental, I., Lingwood, D., Grzybek, M., Coskun, U. & Simons, K. Palmitoylation regulates raft affinity for the majority of integral raft proteins. *Proc. Natl. Acad. Sci. USA* **107**, 22050–22054 (2010).
20. Johnson, S.A. *et al.* Temperature-dependent phase behavior and protein partitioning in giant plasma membrane vesicles. *Biochim. Biophys. Acta* **1798**, 1427–1435 (2010).
21. Veatch, S.L. *et al.* Critical fluctuations in plasma membrane vesicles. *ACS Chem. Biol.* **3**, 287–293 (2008).
22. Lingwood, D. & Simons, K. Detergent resistance as a tool in membrane research. *Nat. Protoc.* **2**, 2159–2165 (2007).
23. Roper, K., Corbeil, D. & Huttner, W.B. Retention of prominin in microvilli reveals distinct cholesterol-based lipid micro-domains in the apical plasma membrane. *Nat. Cell Biol.* **2**, 582–592 (2000).
24. Schuck, S., Honsho, M., Ekroos, K., Shevchenko, A. & Simons, K. Resistance of cell membranes to different detergents. *Proc. Natl. Acad. Sci. USA* **100**, 5795–5800 (2003).
25. Veatch, S.L. & Keller, S.L. Separation of liquid phases in giant vesicles of ternary mixtures of phospholipids and cholesterol. *Biophys. J.* **85**, 3074–3083 (2003).
26. Veatch, S.L. & Keller, S.L. Organization in lipid membranes containing cholesterol. *Phys. Rev. Lett.* **89**, 268101 (2002).
27. Dietrich, C. *et al.* Lipid rafts reconstituted in model membranes. *Biophys. J.* **80**, 1417–1428 (2001).
28. Levental, I., Grzybek, M. & Simons, K. Raft domains of variable properties and compositions in plasma membrane vesicles. *Proc. Natl. Acad. Sci. USA* **108**, 11411–11416 (2011).
29. Keller, H., Lorizate, M. & Schwille, P. PI(4,5)P2 degradation promotes the formation of cytoskeleton-free model membrane systems. *Chemphyschem* **10**, 2805–2812 (2009).
30. Holowka, D. & Baird, B. Structural studies on the membrane-bound immunoglobulin E-receptor complex. 1. Characterization of large plasma membrane vesicles from rat basophilic leukemia cells and insertion of amphipathic fluorescent probes. *Biochemistry* **22**, 3466–3474 (1983).
31. Kaiser, H.J. *et al.* Molecular convergence of bacterial and eukaryotic surface order. *J. Biol. Chem.* **286**, 40631–40637 (2011).
32. Ayuyan, A.G. & Cohen, F.S. Lipid peroxides promote large rafts: effects of excitation of probes in fluorescence microscopy and electrochemical reactions during vesicle formation. *Biophys. J.* **91**, 2172–2183 (2006).
33. Owen, D.M., Rentero, C., Magenau, A., Abu-Siniyeh, A. & Gaus, K. Quantitative imaging of membrane lipid order in cells and organisms. *Nat. Protoc.* **7**, 24–35 (2011).
34. Farkas, E.R. & Webb, W.W. Precise and millidegree stable temperature control for fluorescence imaging: application to phase transitions in lipid membranes. *Rev. Sci. Instrum.* **81**, 093704 (2010).
35. Nikolaus, J. *et al.* Hemagglutinin of influenza virus partitions into the nonraft domain of model membranes. *Biophys. J.* **99**, 489–498 (2010).
36. Kim, H.M. *et al.* A two-photon fluorescent probe for lipid raft imaging: C-laurdan. *Chembiochem.* **8**, 553–559 (2007).
37. Kaiser, H.J. *et al.* Order of lipid phases in model and plasma membranes. *Proc. Natl. Acad. Sci. USA* **106**, 16645–16650 (2009).
38. Shogomori, H. *et al.* Palmitoylation and intracellular domain interactions both contribute to raft targeting of linker for activation of T cells. *J. Biol. Chem.* **280**, 18931–18942 (2005).
39. Kahya, N., Brown, D.A. & Schwille, P. Raft partitioning and dynamic behavior of human placental alkaline phosphatase in giant unilamellar vesicles. *Biochemistry* **44**, 7479–7489 (2005).
40. Bacia, K., Schuette, C.G., Kahya, N., Jahn, R. & Schwille, P. SNAREs prefer liquid-disordered over 'raft' (liquid-ordered) domains when reconstituted into giant unilamellar vesicles. *J. Biol. Chem.* **279**, 37951–37955 (2004).
41. Baumgart, T., Hunt, G., Farkas, E.R., Webb, W.W. & Feigenson, G.W. Fluorescence probe partitioning between Lo/Ld phases in lipid membranes. *BBA—Biomembranes* **1768**, 2182 (2007).
42. Bacia, K., Scherfeld, D., Kahya, N. & Schwille, P. Fluorescence correlation spectroscopy relates rafts in model and native membranes. *Biophys. J.* **87**, 1034–1043 (2004).